Preparation of PTFE-TIO$_2$-GO/EP superhydrophobic costing and its performance study

Y. Chen [a], X. H Xu [b], C. Q. Li [a,*], J. C Yang [c], P. Lv [c], Q. H. Jin [c], G. Q Xu [a], A. Amirfazli [d]

[a] *School of Materials Engineering, Jiangsu University of Technology, Changzhou, 213001, P. R. China*

[b] *College of Preschool Education,Yuzhang Normal University,Nanchang 330103,China*

[c] *Jiangsu Bestfull Technology Co.,LTD,Changzhou, 213300, China*

[d] *Department of Mechanical Engineering, York University, Toronto, ON, M3J 1P3, Canada*

For many years, the issue of microbial adhesion has presented difficulties in both daily life and business. In this paper, superhydrophobic coatings were produced by adding epoxy resin (EP), butyl acetate, titanium dioxide (TiO_2) nanoparticles, polytetrafluoroethylene micropowder (PTFE), and graphene oxide (GO) sequentially into a mug and mixing well, and then modifying the microscopic particles by using perfluorooctyltriethoxysilane (POTS), and lastly producing the superhydrophobic coatings applied via spraying on the aluminum sheet surface. The micro morphology of the samples was analysed by SEM and EDS, the molecular makeup of the samples was analysed by FTIR and the molecular stability, mechanical stability and algae resistance were tested, and finally the the rust unwillingness of the coatings was investigated by using an electrochemical workstation (Tafel and EIS). The outcomes demonstrated that the best GO to nanoparticle mass ratio of 10% was chosen to achieve a contact angle of 167.5° and a sliding angle of 2.5°. The coating contact angle was still superior to 150° after 7 days of immersion in strong acids and bases as well as 3.5 wt% Nacl and after 8 hours of immersion in boiling water. After 800 abrasion tests the contact angle was still 150.6°. Algae resistance tests showed that the coatings had good resistance to algae adhesion.

(Received August 5, 2024; Accepted October 11, 2024)

Keywords: Superhydrophobic, Graphene oxide, PTFE, TiO_2, Anti-algae

1. Introduction

Bio-adhesion is widespread and has a serious impact on people's lives. In international trade, ships are the largest freight carrier in international trade. However, because ships are immersed in seawater for a long time, they are not only corroded by seawater, but also adhered and eroded by

* Corresponding author: cql6660607@163.com

https://doi.org/10.15251/DJNB.2024.194.1481

marine microorganisms, shells, algae and other organisms, which leads to the fouling of their hulls, increase in resistance, and huge energy consumption [1-5]. The properties of lotus leaves provide inspiration for the study of superhydrophobic surfaces, whose low contact area and self-cleaning properties have significant potential in resisting biological adhesion.

Low surface energy and roughness are essential for construct superhydrophobic appears [6-8]. Based on the two factors scientific researchers drilled many preparation methods: etching [9-10], sol-gel [11-13], templating [14-16], electrochemical deposition [17], hydrothermal [18], spraying [19-20], and self-assembly [21-23]. Over the previous few decades, nano-oxides have been broadly adopted for the construction of superhydrophobic coatings due to their special and beneficial qualities. Among them, titanium dioxide (TiO_2) nanoparticles, among the subjects that has been researched the most, have been widely used in photocatalysis and coatings due to their excellent antioxidant properties, aging resistance,rich content, cheap cost, and strong thermal stability.Most notably, numerous research have revealed that antimicrobial metal oxides (TiO_2) have anti-bioadhesion effects [24-26]. PTFE micropowders have been extensively employed in coating materials because of their excellent chemical endurance, excellent temperature resistance and minimal friction [27]. Graphene oxide (GO), on the other hand, has become a popular material within the domain of anticorrosive coatings because of its vast appear area, excellent compatibility and excellent barrier properties [28-31].

For this reason, in this paper, the PTFE-TiO_2-GO/EP superhydrophobic coating was obtained through a single-step spraying process. The microscopic morphology of the samples was analyzed by SEM and EDS,as well as the chemical makeup of the samples was examined by FTIR, etc. The effect of the mass ratio of GO to nanoparticles and other factors about the wettability of the coatings was explored. The chemical and mechanical steadiness of the coatings were examined, and the coatings were tested for algae resistance.

2. Experimental

2.1. Materials

Epoxy resin (EP, E51) was purchased from Guangzhou Suixin Chemical Co. Curing agent (D230) was purchased from Shandong Jingshun Chemical Co. Perfluorooctyltriethoxysilane (POTS, analytically pure) was purchased from Guangdong Qianjin Chemical Reagent Co. γ-aminopropyltriethoxysilane (KH550) was purchased from Shandong Bosheng Chemical Co. Butyl acetate, hydrochloric acid (HCl), sodium hydroxide (NaOH), sodium chloride (NaCl), all analytically pure, were purchased from Sinopharm Chemical Reagent Co. Nano TiO_2 (30 nm) was purchased from Shandong Yusuo Chemical Technology Co. Polytetrafluoroethylene micropowder (PTFE, 1.6 μm) was purchased from Shanghai Jujia Plastic Material Co. Graphene oxide (GO) was purchased from Zhejiang Zhitian Nanomicro New Material Co. Chlorella species and culture medium were purchased from the Green Water Conditioning Store.

2.2. Preparation process

2.2.1. Substrate (Al) pretreatment

Aluminum sheet was utilized as the coating's substrate. Using 300 grit sandpaper, the aluminum sheet was first sanded in various directions. It was then washed with deionized water and dried for spare.

2.2.2. Preparation of superhydrophobic coatings

First, 3.3 g of epoxy resin was uniformly dispersed into 25 g of butyl acetate solvent, ultrasonically shocked and dispersed for 20 min, and then magnetized at 400 r/min for 1 h, to acquire a homogeneously scattered mixture. Next, 2.4g TiO_2, 0.6g PTFE, 0.2g KH550 and a specific quantity of GO were incorporated in the above fluid, ultrasonically shocked and dispersed for 20min, and then magnetically stirred at a speed of 400r/min for 1h, and a homogeneously dispersed mixed solution was obtained. Finally, 0.4 g of POTS and 1.1 g of curing substance were incorporated in the mixed fluid, which was agitated magnetically at 400 r/min for 3 h to acquire a homogeneously distributed mixture. The combination remedy was sprayed onto the aluminum sheet using a single spraying procedure, and the coating was cured at room temperature for 24h after spraying to produce the PTFE-TiO_2-GO/EP superhydrophobic coating. Fig.1 depicts the schematic for preparation.

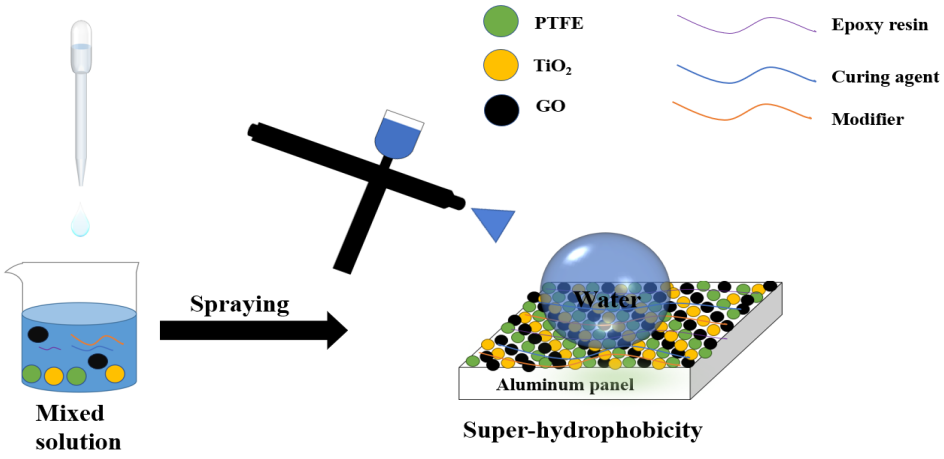

Fig. 1. Schematic diagram of the preparation of PTFE-TiO_2-GO/EP superhydrophobic coating.

2.3. Characterization and performance testing of samples

The contact angle (CA) and roll angle (SA) values of the coated surfaces were tested by a contact angle tester (Krüss, DSA 30).The test platform held the samples.Subsequently, 10 microliters of deionized water were applied to the samples' surface and given a minute to stabilize.Then the CA and SA were measured, and the average of the five parallel tests was taken as the test results. A scanning electron microscope with thermal field emission (SEM, QUANTA FEG 400, FEI, USA) was used to analyze the micro-morphology of the samples. Using an energy spectrometer, the samples' surface elements were examined (EDS, GENESIS, EDAX, USA). Using Fourier transform infrared spectroscopy, the hydrophobically modified nanoparticles were examined(FTIR, Nicolet iS5, Thermo Fisher Nicholson, USA).

Chemical stability test: Soak the samples in different pH solutions and NaCl (3.5wt%) solutions,remove them on a regular basis to clean the surface with deionized water, dry them, and then test the modifications in the wettability of the sample surface.

Abrasion Resistance Test: The abrasion opposition to the samples was tested on a steel wool scuff tester in which the samples were placed on 1000 grit sandpaper and subjected to 100 g weight. After that, the samples underwent 40 ablations per minute over a 10 cm length.

Adhesion test: In accordance with the international standard "Paint and varnish - Cross-cutting test" (ISO2409-2013), the superhydrophobic coating was scratched by a pug knife to form a grid pattern with a spacing of 2mm. Subsequently, the tape was applied to the surface of the grid pattern, and after 5 min, the tape was slowly removed.

Self-cleaning and antifouling test: The self-cleaning effect of the sample surface is evaluated by testing the ability of rolling water droplets to carry simulated contaminant particles. The antifouling performance of the sample is assessed by immersing the sample in a contaminant solution and observing the presence of the contaminant solution on the sample surface.

UV Aging Test: The sprayed coating is placed in a UV accelerated aging tester (maximum radiation wavelength of 313nm, power 30w, vertical distance of the sample from the light source down to 10cm) for 70 hours of irradiation. The contact angle as well as the rolling angle of the coating are measured at regular intervals, and the UV resistance of the coating is evaluated by taking measurements at 5 different positions of the coating and averaging these values as the test value.

Grit Impact Test: The grit impact test is performed by impacting the appear of the coating with 30 g of grit less than 1 mm in diameter. First, the coating and horizontal plane are kept at a 45° angle. The sand particles are then placed into a funnel, and one cycle is created by allowing the sand to descend vertically from a height of 30 cm above the coating. After every 3 impact cycles, the wettability of the coating was measured.

Heat resistance test: For three hours, the coating is heated to 100, 150, 200, 250, and 300 degrees Celsius in a muffle furnace, then removed and cooled for 1 hour, then CA and SA are measured.

Scorch test: Fix the coating on top of the alcohol lamp through the iron frame, then ignite the alcohol lamp to scorch the coating, wait for a period of time after burning, remove and cool down for 1 hour, and then test the wettability and antifouling performance of the coating.

Boiling water treatment test: Immerse the coating in boiling water, remove the coating with tweezers at regular intervals, then place it in an electric blast drying oven, and when the coating is dry, remove it and test the wettability of the coating.

Anti-algae test: Chlorella vulgaris was chosen as the test algae. Two milliliters of culture medium and 100 milliliters of algae species were added into a glass container and incubated at room temperature. After that, the samples were submerged in the algal water and taken at intervals to observe the adherence status of Chlorella under a body microscope.

3. Results and discussion

3.1. Effect of GO addition on coating wettability

To ascertain the impact of various contents of GO particles on superhydrophobicity, we prepared different coatings by changing the GO particle content. As observed from Fig. 2, when the

content of GO and nanoparticles is 2%, CA is 146.3° and SA is 15.2°, which meets the hydrophobicity requirement, but does not meet the superhydrophobicity standard. With the increase of GO content, CA is increasing and SA is decreasing, and when the GO content is elevated to 10%,SA drops to 2.5° while CA hits a top of 167.5°. This is attributed to the dense stacking of GO particles providing a rich surface structure and the pores are essential for superhydrophobicity, which enhances the superhydrophobicity. Continuing to increase the GO content, a slight decrease in CA was found. This is due to the fact that as the proportion of GO particles in the coating gradually increases, the content of EP as a binder correspondingly decreases, which loosens the coating structure and leads to reduced stability. Therefore, the GO to nanoparticle mass ratio of 10% was selected as the best for economic and practical reasons.

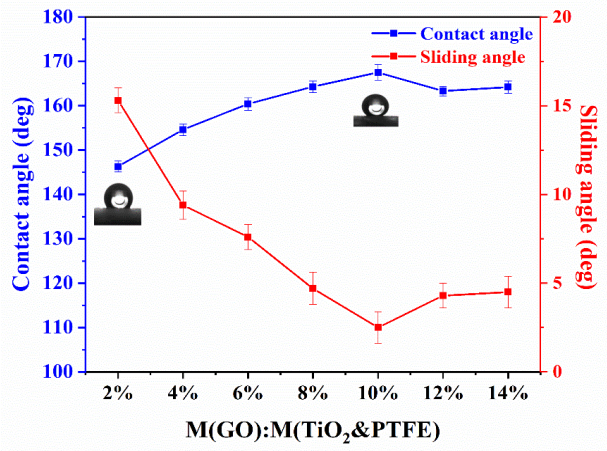

Fig. 2. Effect of GO to nanoparticle mass ratio on hydrophobicity of coatings.

3.2. Surface morphology and chemical composition analysis

The Fourier transform infrared spectroscopy was used to evaluate the chemical composition of the composite coating. Although nano-TiO2 can provide nanostructures, it needs to be modified due to its high surface energy as well as its ease of aggregation.KH550 utilizes the hydrophilicity of -NH2, which can lead to a better dispersion of inorganic materials in butyl acetate. And POTS can effectively reduce the surface energy of titanium dioxide nanoparticles by taking advantage of the high fluorine content and long carbon chain. The FTIR of the modified nanoparticles is shown in Fig. 3, and the spectral line f is a C-F stretching vibration peak at 1202.58 cm-1 and 1145.31 cm-1, in the form of C-F2 bond or C-F3 bond. The spectral lines a and b do not change much because the C=C covalent bond that constitutes GO is the most stable chemical bond in nature, and there is no chemical reaction between GO and the modifier at room temperature, so no new functional group is generated. Compared with the spectral line c, the spectral line d shows the Si-O-Si band of KH550 at 1066.4 cm-1 and the characteristic peaks of C-F in POTS near 1241.3 cm-1 and 1144.1 cm-1, indicating that the nano-TiO2 was successfully modified by KH550 and POTS.

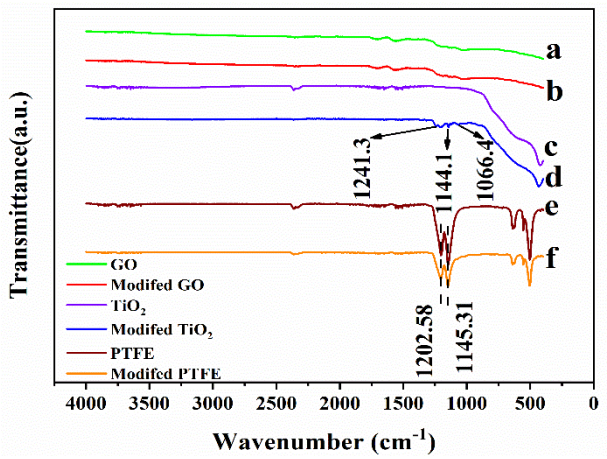

Fig. 3. Fourier infrared spectroscopy test plot.

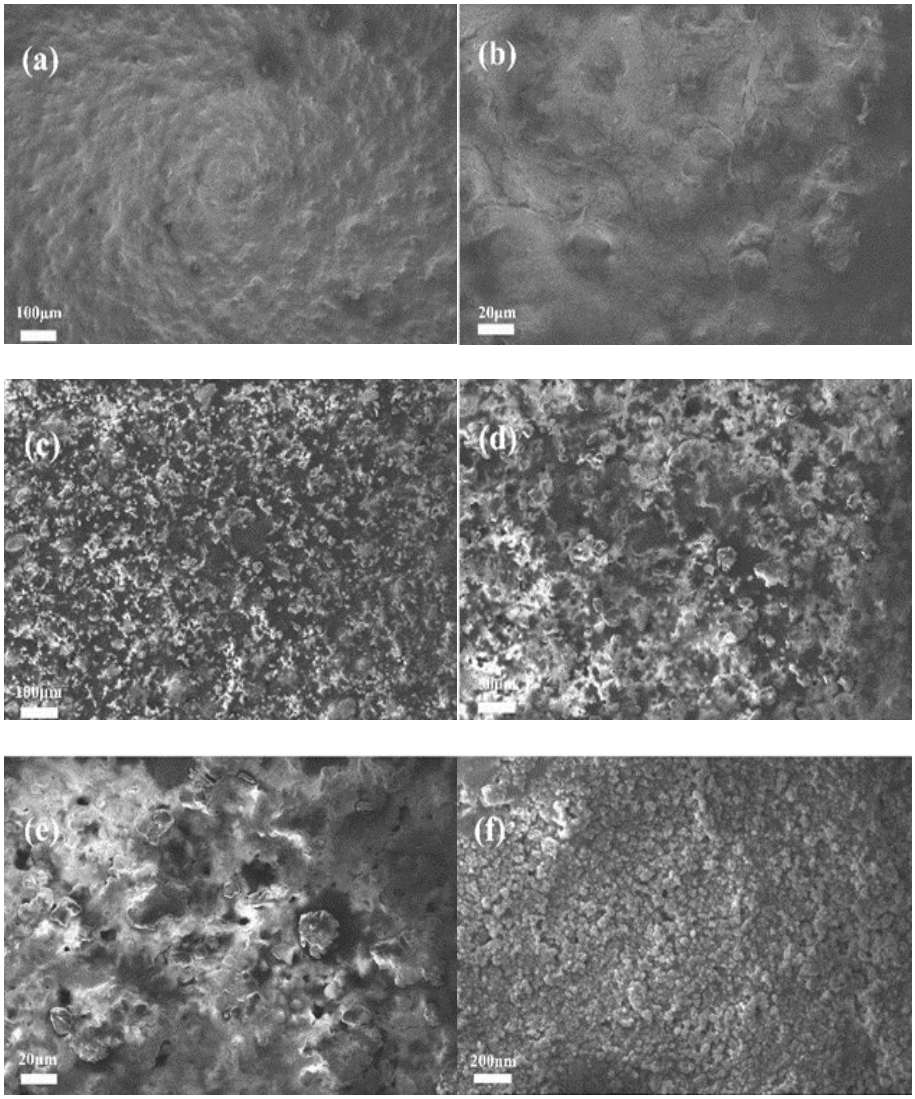

Fig. 4. SEM images of different coatings; (a-b) SEM images at 2% GO content; (c-f) SEM images at 10% GO content.

The appear micromorphology of the coating was analyzed via electron scanning microscopy. As demonstrated in Fig. 4 (a-b), when the content of GO is 2%, the micro- and nano-rough structures are almost completely covered by the epoxy resin, thus affecting the coating's hydrophobic appear and preventing the coating from achieving superhydrophobicity. From Fig. 4(c-f), It is evident that by continuing to raise the GO content, a large number of micro-nanometer coarse architecture exist on the coating's appear when the content of GO is 10% compared to that of Fig. 4(a-b).The micro-nanometer-sized papillae on the coating's appear the coatings make the hydrophobicity of the coatings significantly enhanced, and these rough structures are able to form an air layer, which confers the surface with excellent superhydrophobicity.

As shown in Fig. 5, the surface elements of the superhydrophobic coating contain Ti, Si, C, O, and F, whose percentages are 26.0%, 0.8%, 27.2%, 35.7%, and 10.3%, respectively.The primary source of the C element is PTFE micropowder and graphene oxide, the Ti element primarily comes from nano-TiO2,the primary sources of the F element are POTS and PTFE micropowder. POTS and KH550 are the two coupling agents that provide the majority of the Si element, and O element is mainly from nano TiO2 and graphene oxide, which fits the arrangement of PTFE-TiO2-GO/EP superhydrophobic coatings, making the elements evenly dispersed across the coatings.

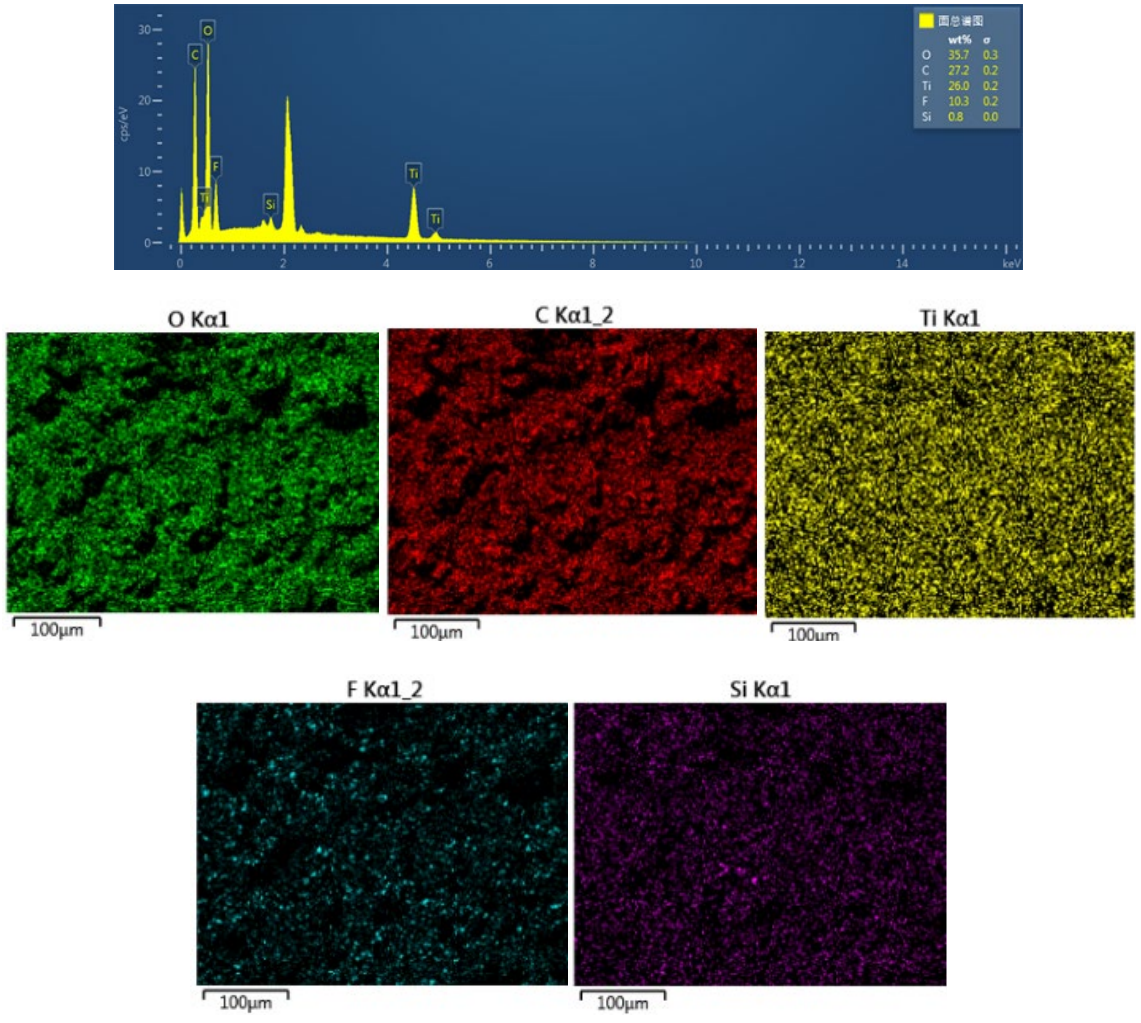

Fig. 5. Dispersion of superhydrophobic coating elements.

3.3. Coating durability tests

The durability of superhydrophobic coatings is an important factor since the coatings spend a lot of time outside. For this reason, the durability of the samples was tested in several harsh environments (PH=1 solution, PH=14 solution, 3.5 wt.% NaCl solution, boiling water treatment, sand impact test, adhesion test, heat resistance test, abrasion test, alcohol lamp burn test, and UV aging test).

When superhydrophobic coatings are exposed to their surroundings, they are frequently exposed to various acidic and alkaline liquids, including alkaline solutions, acid rain, and salt water. As shown in Fig. 6 (a-d), they are the connection of hydrophobicity plots of the coatings immersed in 3.5 wt.% NaCl aqueous solution, powerful alkali (PH=14), powerful acid (PH=1), and boiling water for different times, respectively. From Fig. 6 (a-c), It is evident that the CA of the coatings is still greater than 150° following a 7-day soak in 3.5 weight percent NaCl, strong acid, and strong alkali corrosive solution,which suggests that the specimens have good chemical stability in acid and alkali salt solutions. As observed in Fig. 6(d), after the coatings were treated with boiling water for 8 h, the CA was above 150° and the SA was below 10°, demonstrating that the samples still had good stability in boiling water as well.

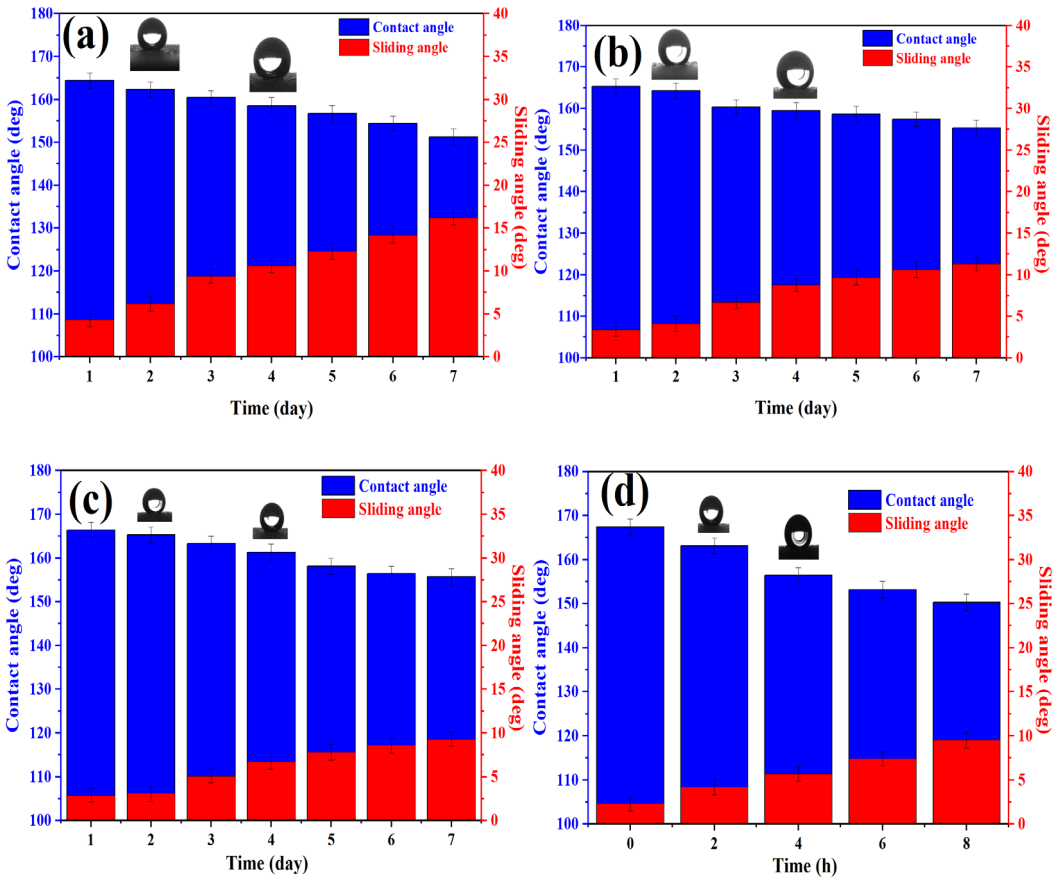

Fig. 6. Chemical stability tests; (a) NaCl (3.5 wt%) solution; (b) PH= 14 solution; (c) PH= 1 solution; (d) boiling water.

This is mostly because of the micro/nanostructure and chemical inertness of the components in the superhydrophobic coating, which prevented the corrosive solution from penetrating into the coating. Meanwhile, Zhao et al [32] demonstrated that the ability to withstand corrosion of AZ31 Mg alloy could be notably enhanced by adding GO to the electrolyte for plasma electrolytic oxidation (PEO).GO played a barrier role, effectively preventing the aggressive electrolyte from contacting the metal surface and increasing the degree of zigzagging in the diffusion path of the electrolyte.The silylated coatings containing GO covered on Mg also exhibited enhanced resilience against corrosion, which was mainly credited with the impermeability of GO to the diffusion of ions in corrosive solutions [33]. In addition, the superhydrophobic surface, due to its excellent water repellent properties, was able to form an air layer between the corrosive liquid and the coated surface, thus further hindering the penetration of corrosive ions and providing more comprehensive protection [34]. The chemical stability of the coating was greatly enhanced compared to the PTFE@TiO2/EP superhydrophobic coating.

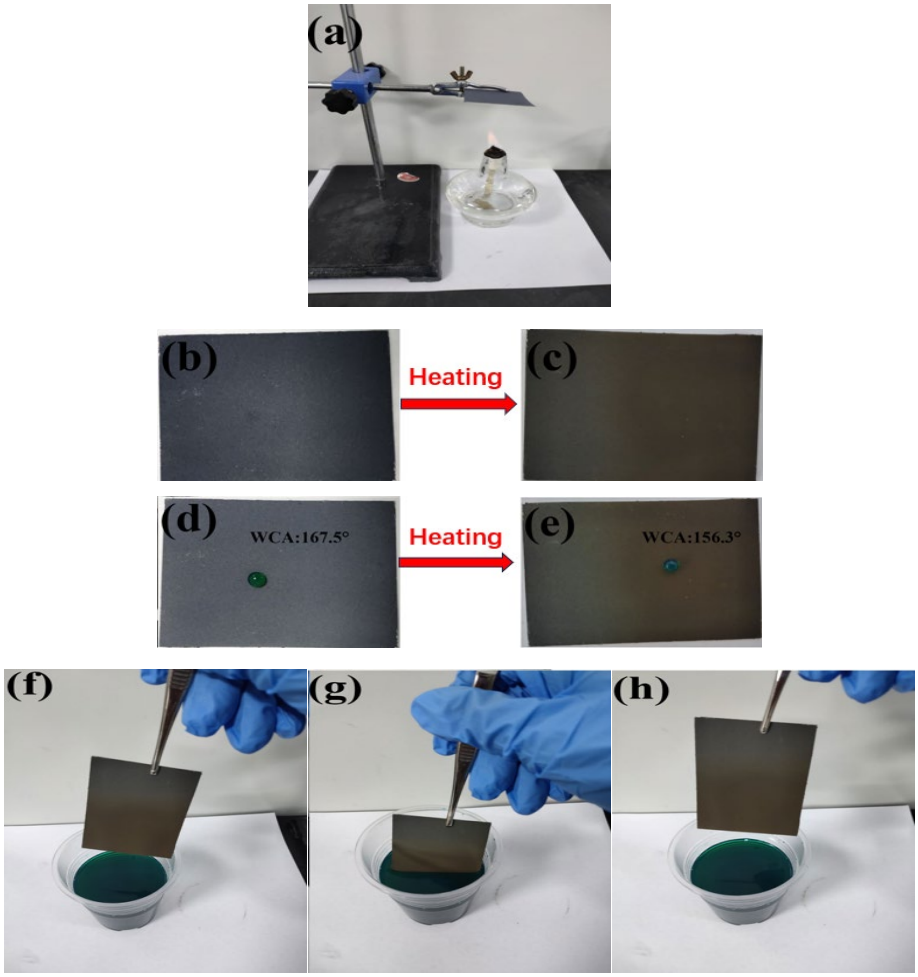

Fig. 7. Scorch test of samples. (a) Schematic diagram of heating by alcohol lamp; (b) and (c) diagrams ofalterations to the coating's surface state before and after heating; (d) and (e) schematic diagrams of the coated surface's water contact angle before and after heating; (f-h) antifouling process of the superhydrophobic coatings after cauterization.

Meanwhile, the heat resistance of the coatings as well as the UV aging resistance were explored. The wettability changes of the samples at different temperatures are displayed in Fig. 8(a). As illustrated in Fig. 8(a), the CA of the superhydrophobic coatings was greater than 155° across the whole temperature range,demonstrating that the PTFE-TiO2-GO/epoxy superhydrophobic coatings have excellent heat resistance. Since the coating is directly exposed to the natural environment, it will inevitably be subjected to UV radiation, therefore, the UV aging test was conducted on the sample through the UV aging tester, and As may be observed from Figure 8(b) that after 70 hours of irradiation, the UV irradiation did not lead to a noteworthy decline in the contact angle or a significant raise in the rolling angle of the coating, and the wettability did not change significantly, which It suggests that the coating performs exceptionally well when it comes to UV aging.

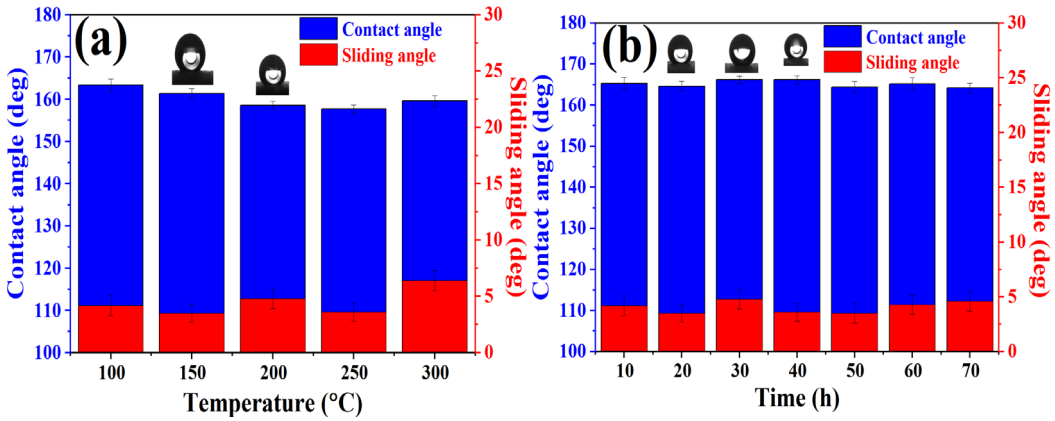

Fig. 8. (a) Heat resistance test; (b) UV aging test.

The samples were subjected to sand impact tests to assess their robustness as demonstrated in Fig. 9. From Fig. 9(a),it is evident that the CA of the PTFE-TiO2-GO/epoxy superhydrophobic coating is decreasing and the SA is increasing as the number of sand impacts keeps growing. The contact angle of the coating after 18 sand impacts was 151.3°, and the rolling angle was 12.4°, which still achieved the superhydrophobic effect, demonstrating that the PTFE-TiO2-GO/epoxy resin superhydrophobic coating has good mechanical stability. The main reason for the reduce in contact angle is credited with, initially, abrasion damage due to sand particle influence on the micro- and nanostructures of the coating appear. Additionally, it is possible that some sand particles remain on the coating surface and bring hydrophilic groups.

In practical applications,the consistency of the coating to the foundation is one of the elements to be considered for superhydrophobic coatings. The adhesion of the PTFE-TiO2-GO/epoxy superhydrophobic coating was tested based on the global norm "Paint and varnish - Cross-cut test" (ISO2409-2013). As can be seen from Figure 10(c), the cuts were smooth, there was no flaking in the compartments or at the edges of the cuts, and there was only a little quantity of powder adhering to the tape. From Fig. 10(d), It is evident that after tape peeling, the superhydrophobic coating still has good wettability. Concerning the assessment of the worldwide standard test outcomes in Fig. 10(e), the adhesion of the coating attains the greatest grade of 0, indicating that the superhydrophobic coating has excellent adhesion properties.

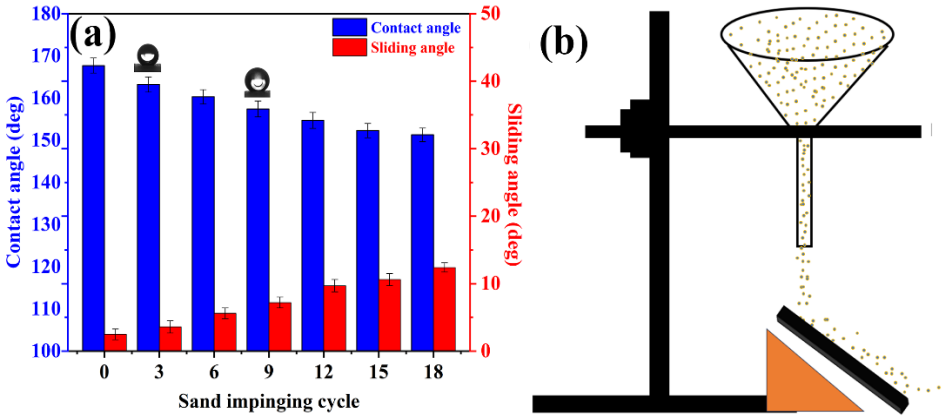

Fig. 9. (a) Variation of the wettability of the samples with sand impact cycles; (b) Schematic diagram of sand impacts.

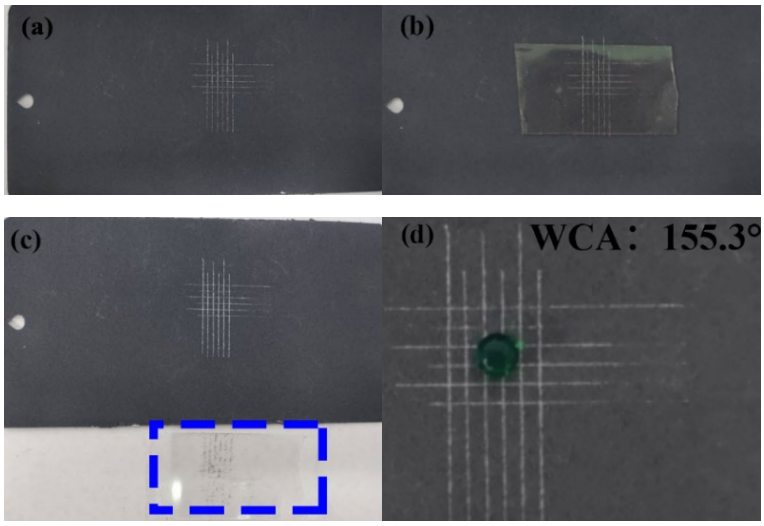

(e)

Grade	Illustration	Surface appearance of criss-cross cut areas that have fallen off
0	The cutting edge is completely smooth, and there is no falling off.	—
1	A little coating peeled off at the cut intersection. The cross-cut area should not be affected by more than 5%.	
2	Coating peeling off cut edges and/or intersections. The affected cut area is greater than 5% but less than 15%.	

Fig. 10. (a) The orthogonal grid is being constructed on the surface of the coating with a palletizer; (b) the tape is applied to the surface of the orthogonal grid; (c) the tape is removed and there is a small amount of powder on the tape; (d) wetting diagram of the coating after the tape is removed; (e) International Standard for Paints and Varnishes - Cross-cutting Tests (ISO2409-2013).

The connection between the quantity of rubbing of the samples and wettability and the changes in SEM of the sample surface after rubbing are shown in Fig. 11. It can be obtained from Fig. 11 that the number of sandpaper rubbing has a noteworthy impact on the hydrophobicity of the coating. From Fig. 11(a), it can be obtained that when the number of rubbings grows, CA declines, when the coating is abraded by 800 times of sandpaper abrasion, the CA of the superhydrophobic coating decreases from 167.5° to 150.6°, and the SA increases from 2.5° to 24.7°, and the coating still has a better superhydrophobicity,just that the rolling angle is more than what's needed. When the coating was worn for more than 1200 times, the hydrophobicity of the sample decreased, CA was 143.5° and SA was 33.2°, at this time, the CA was lower than 150°, the coating did not have superhydrophobicity, but the coating still had good hydrophobicity.

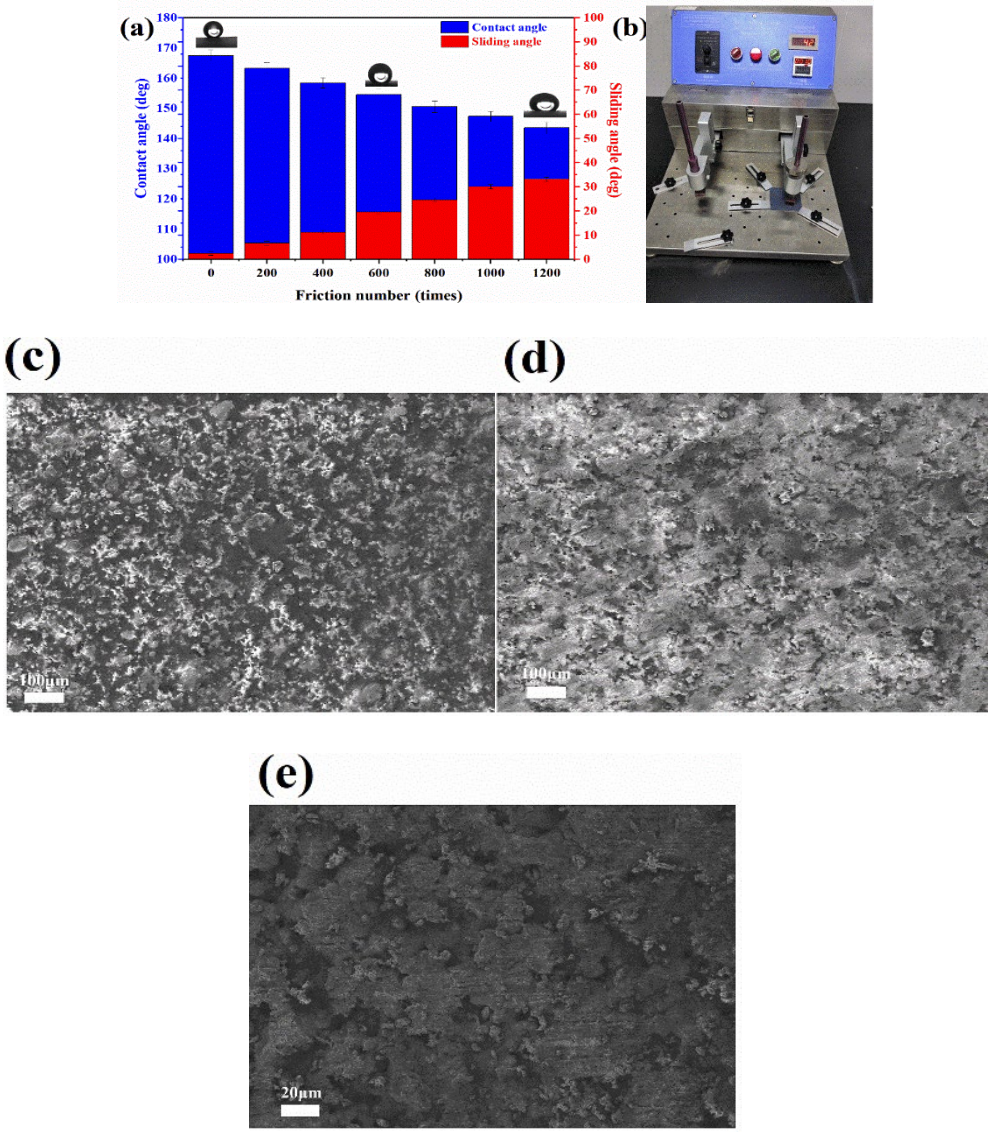

Fig. 11. (a) Sample friction number versus wettability; (b) Friction schematic; (c) Scanning electron microscopy of superhydrophobic coating; (d-e) Scanning electron microscopy of the sample after 1200 friction cycles.

Comparing the low magnification Fig. 11 (c) and low enlargement Fig. 11 (d), it is evident that after 1200 times of friction, there are obvious friction traces on the appear of the coating, most of the coating is rubbed off, and the whole surface of the coating becomes smoother, and at this time, it is difficult to maintain the superhydrophobicity of the coating only by relying on the low-surface-energy substances on the appear of the coating. From the high magnification Figure 11(e), it can be observed that although after friction, the coating surface still has micro-nanometer rough structure, indicating that the sample exhibits strong friction opposition. The main reason for the coating's excellent abrasion resistance is that the micro-nanostructures are more abrasion-resistant than the single-layer nanostructures [35]. Secondly, The robust adherence of the EP itself enhances the cross-linking between the particulate materials and also improves the bonding effect with the substrate. Meanwhile, the addition of nanoparticles also makes this effect more significant, with a tighter cross-linking structure between the substances and better performance, which is not easy to be worn off. In addition, GO has been shown to significantly improve the coatings' mechanical characteristics[36]. Compared with the PTFE@TiO2/EP superhydrophobic coating, the abrasion resistance of this coating was significantly improved.

3.4. Self-cleaning and antifouling performance tests

Adhesion of pollutants on car windshields, skyscraper curtain walls, photovoltaic equipment and solar panels has a negative impact on daily life. And the self-cleaning property is another characteristic of superhydrophobic surfaces. Ordinary yellow pigment was used as a simulated pollutant to test the self-cleaning property of different samples, and the test findings are displayed in Fig. 12. From Fig. 12 (a1-a3), it can be observed that the ordinary yellow pigment still adheres to the appear of the Al after the dripping water are applied to the surface. However, as demonstrated in Fig. 12 (b1-b3), when the dripping water were applied on the superhydrophobic surface, the water droplets could thoroughly clean the ordinary yellow pigment on the path of the superhydrophobic surface and the surface was thoroughly cleaned. It demonstrates that the PTFE-TiO2-GO/epoxy superhydrophobic coating has excellent self-cleaning performance.

Figure 13 shows the antifouling process of the PTFE-TiO2-GO/epoxy superhydrophobic coating. The antifouling performance of the aluminum sheet and the coating were tested separately using cobalt green aqueous solution as a simulated contamination source. Figure 13 (a1-a4) shows that the aluminum sheet was soaked in the cobalt green watery solution and eliminated, from which it can be seen that many green pollutants adhered to the appear of the Al after removal. From Fig. 13 (b1-b4), It is evident that the ordinary coating surface is the same as the appear of the Al, the surface is adhered by the pollutants and does not have antifouling properties. In contrast, Fig. 13 (c1-c4) demonstrates that the PTFE-TiO2-GO/EP superhydrophobic coating was immersed in a cobalt green aqueous solution and removed, and it can be seen that the appear of the superhydrophobic coating remained clean and dry without any contaminant adherence after the removal of the coating. It indicates that the prepared coating has outstanding antifouling performance. This is due to the construction of a multiscale micro- and nanostructure on the coating surface, which is capable of trapping a stable air layer, thus forming a shielding layer and effectively preventing the penetration of contaminants. In addition, this structure reduces the contact area of water droplets with the coating surface and induces the contaminant-containing water droplets to leave quickly.

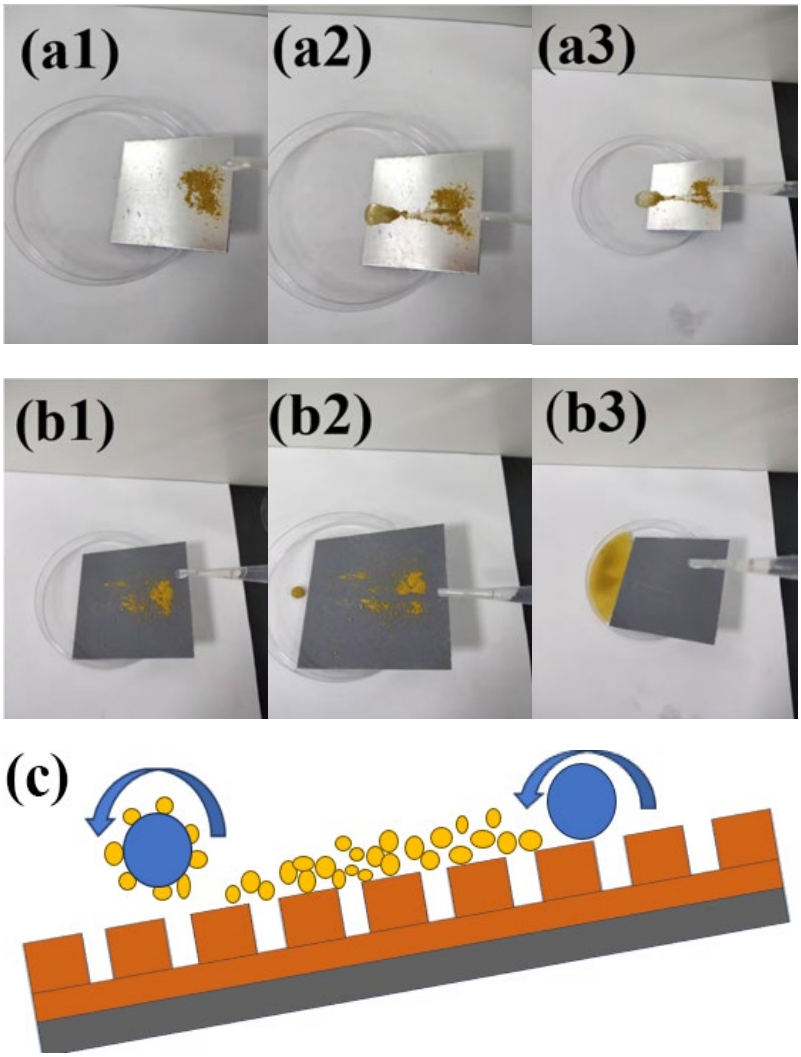

Fig. 12. Self-cleaning test; (a1-a3) self-cleaning test of aluminum sheet contaminated by pigment; (b1-b3) self-cleaning test of superhydrophobic coating contaminated by pigment; (c) shows the self-cleaning mechanism diagram.

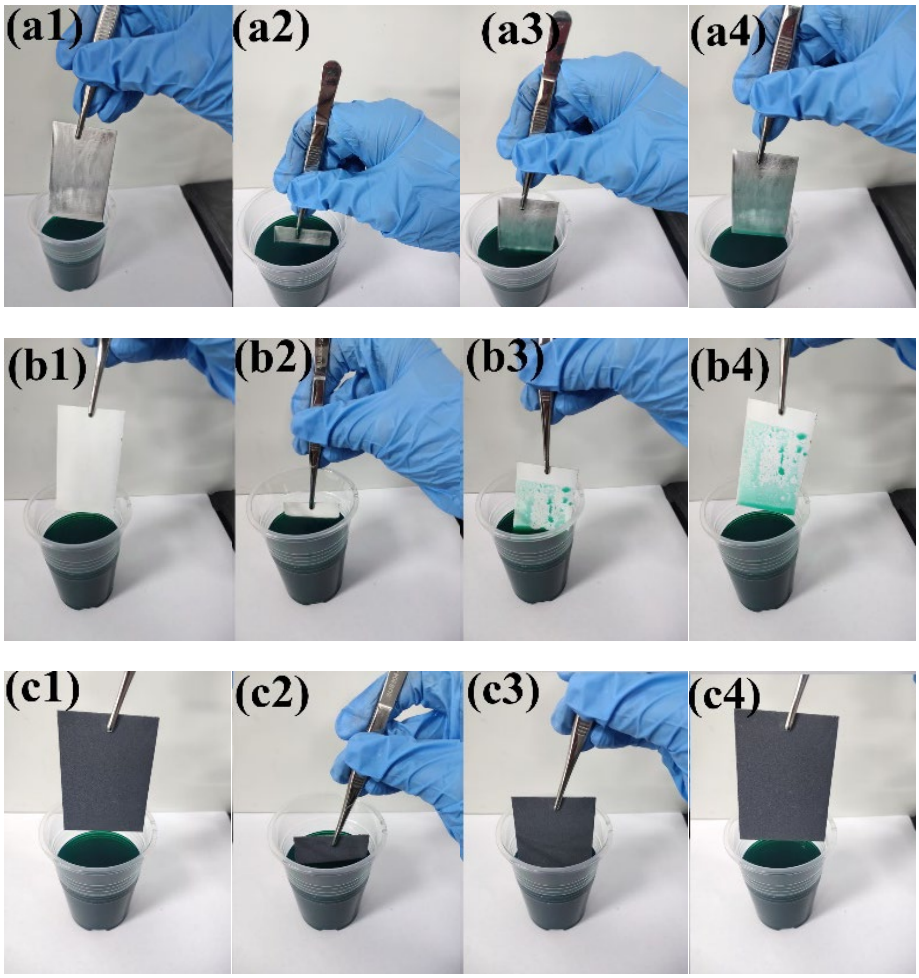

Fig. 13. (a1-a4) Aluminum sheet; (b1-b4) Normal coating; (c1-c4) Superhydrophobic coating antifouling process.

3.5. Algae resistance tests

From Fig. 14, it can be observed that Chlorella adheres most to green algae on the appear of Al and epoxy resin coating with increase in time. After 15 days of immersion, the appear of the Al and epoxy resin coating showed more significant adherence of Chlorella. After 30 days, the amount of Chlorella adhering to the surface increased significantly compared to the first 15 days, and the surface was basically covered by Chlorella. This is because the biofilm formed on the surface in the first 15 days provided nutrients for the adhesion of Chlorella, which further accelerated the adhesion speed of Chlorella. On the other hand, the surface of PTFE-TiO2-GO/epoxy resin superhydrophobic coating had almost no algae adhered on the surface after 15 days of immersion, and only a little quantity of Chlorella adhered on the appear of the coating after 30 days of immersion. From the above analysis, it can be seen that the area of chlorella adhering to the surface of PTFE-TiO2-GO/epoxy superhydrophobic coating is noticeably smaller than that of the remaining samples, demonstrating that the PTFE-TiO2-GO/epoxy superhydrophobic coating has a well performance of anti-algae adhesion.

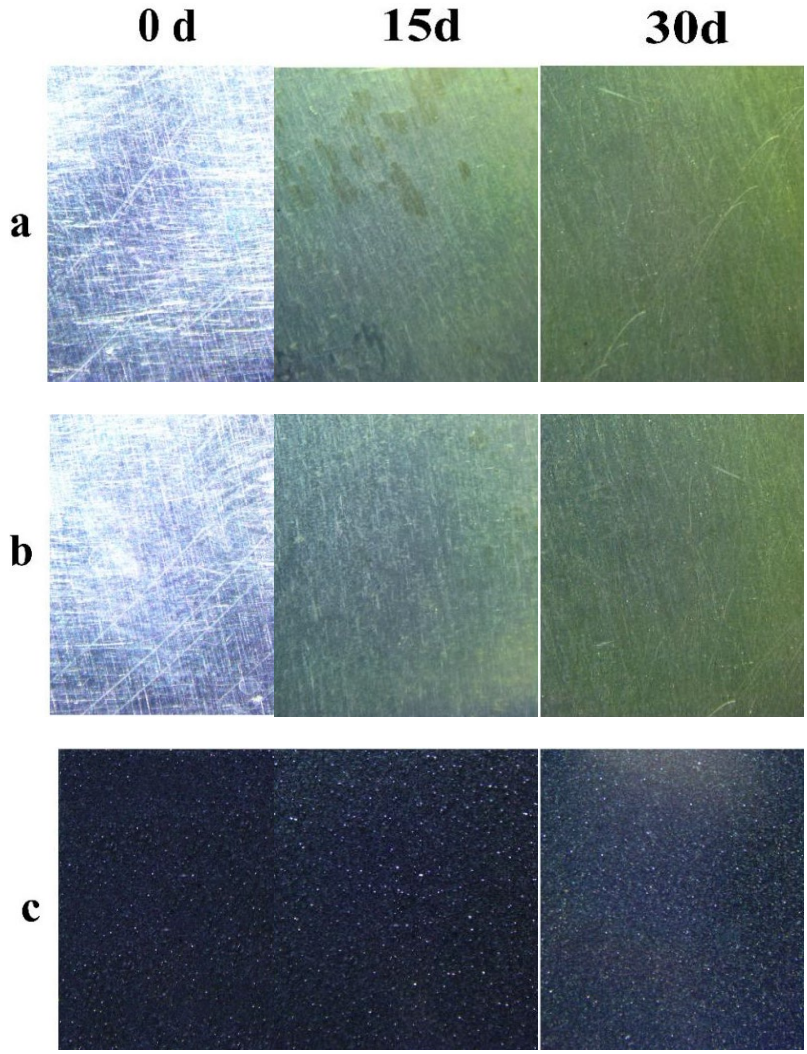

Fig. 14. Volume-viewing microscope diagrams of the surface algal resistance of different samples produced at different times (a, aluminum sheet, b, epoxy coating, c, PTFE-TiO2-GO/epoxy superhydrophobic coating).

3.6. Analysis of anti-algal mechanisms

The anti-algae technique of the PTFE-TiO2-GO/epoxy superhydrophobic coating is shown in Figure 15. From Fig. 15, It is obvious that the superhydrophobic coating has a well anti-algae property compared to the aluminum and epoxy coatings, which is due to the fact that the superhydrophobic coating has a low contact area as well as a low adhesion force, which prevents the adherence of Chlorella on the appear of the coating. On the other hand, the surface of the superhydrophobic coating consists of antimicrobial metal oxide (TiO2 nanoparticles), and it has been shown [37] that the role of metal oxide nanoparticles in preventing biofouling may be based on at least three mechanisms. First, these particles may release bactericidal components into the surrounding environment. Second, interactions on the surface of the particles may produce substances with bactericidal effects. Finally, the nanoparticles or their surfaces may interact directly with the organism target, resulting in the organism's demise. The reason for the good anti-algae effect of the PTFE-TiO2-GO/epoxy superhydrophobic coatings is that the combination of these two aspects sufficiently reduces the adherence of Chlorella on the superhydrophobic coatings' outside.

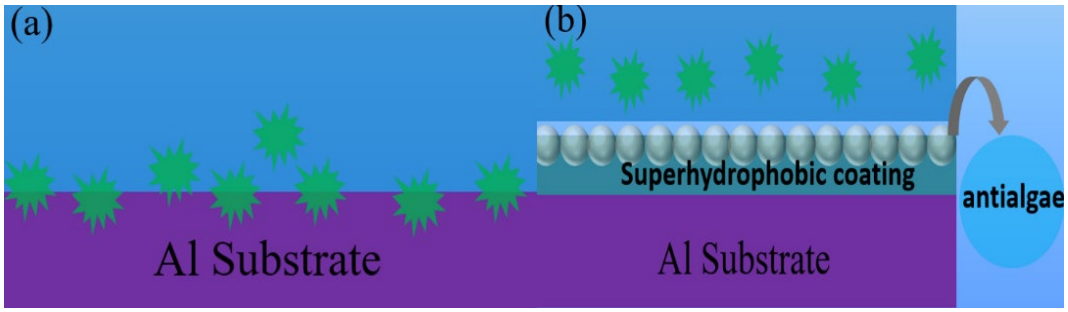

Fig. 15. Algae resistance mechanism; (a) normal coating; (b) superhydrophobic coating.

4. Conclusions

This work describes the preparation of long-lasting PTFE-TiO2-GO/epoxy superhydrophobic coatings using a single-step spraying technique. The findings indicate that the prepared superhydrophobic coatings have outstanding superhydrophobic properties, and the CA can reach 167.5° and the SA can reach 2.5°. The coatings have excellent durability. After 800 abrasion tests, the CA of the coating surface is still larger than 150°; the adhesion test shows that the adhesion of the coating reaches the highest level 0; the coating can still maintain superhydrophobicity after 7 days of soaked in powerful acid (PH=1), powerful alkali (PH=14), and 3.5 wt.% NaCl corrosive solution; after 8 hours of immersion in boiling water, the CA of the coating is still larger than 150°; After 18 times of sand impact, the coating still has superhydrophobicity; after 70 hours of UV aging test, the CA and SA of the coating surface did not change significantly, showing excellent UV opposition; concurrently, the coating also has well heat resistance and self-cleaning properties. The anti-algae results show that after 30 days of anti-algae adhesion test, only a small amount of algae adheres to the prepared PTFE-TiO2-GO/epoxy superhydrophobic coating, which indicates that the coating has good anti-algae adhesion performance.

Acknowledgments

The author thanks the National Natural Science Foundation of China (52073127) and the International Science and Technology Cooperation Project of Changzhou Science and Technology Bureau (CZ20230024) for their funding.

References

[1] Yebra D.M., Kiil S., Dam-Johansen K., Progress in Organic Coatings, 2004, 50 (2): 75-104; https://doi.org/10.1016/j.porgcoat.2003.06.001

[2] Townsin R.L., Biofouling, 2003, 19 (S1): 9-15; https://doi.org/10.1080/0892701031000088535

[3] Dafforn K.A., Lewis J.A., Johnston E.L., Marine Pollution Bulletin, 2011, 62 (3): 453-465; https://doi.org/10.1016/j.marpolbul.2011.01.012

[4] Schultz M.P., Biofouling, 2007, 23 (5-6): 331-341; https://doi.org/10.1080/08927010701461974

[5] Almeida E, Diamantino T C, Sousa O D., Progress in Organic Coatings, 2007, 59(1): 2-20; https://doi.org/10.1016/j.porgcoat.2007.01.017

[6] X. Gao, J. Zhou, R Du, et al., Advanced Materials, 2016,28(1):168-173; https://doi.org/10.1002/adma.201504407

[7] B. Wang, W. Liang, Z. Guo, et al., Chemical Society Reviews, 2015, 44(1):336-361; https://doi.org/10.1039/C4CS00220B

[8] Q. Ma, H. Cheng, A.G. Fan, et al., Special Wettable Materials, 2016,12(16):2186-2202; https://doi.org/10.1002/smll.201503685

[9] Barthwal S, Barthwal S., Surfaces and Interfaces, 2024, 46: 103933; https://doi.org/10.1016/j.surfin.2024.103933

[10] Zhu J, Duan Y., Applied Surface Science, 2024, 648: 159009; https://doi.org/10.1016/j.apsusc.2023.159009

[11] Montheil T, Echalier C, Martinez J, et al., Journal of Materials Chemistry B, 2018, 6(21): 3434-3448; https://doi.org/10.1039/C8TB00456K

[12] Yao X, Zhao W, Zhang H, et al., Colloid and Interface Science Communications, 2023, 57: 100758; https://doi.org/10.1016/j.colcom.2023.100758

[13] Gosiamemang T, Heng J Y., Separation and Purification Technology, 2024, 336: 126185; https://doi.org/10.1016/j.seppur.2023.126185

[14] Li K, Zhang Q, Li J, et al., Journal of Molecular Liquids, 2024, 396: 123922; https://doi.org/10.1016/j.molliq.2023.123922

[15] Shen W, Zhang Z, Xu K, et al., Progress in Organic Coatings, 2024, 189: 108344; https://doi.org/10.1016/j.porgcoat.2024.108344

[16] Zhang X, Wei C, Hao Y J, et al., Chemical Engineering Science, 2023, 282: 119325; https://doi.org/10.1016/j.ces.2023.119325

[17] Zhao Y, Suo L, Zhang S, et al., Colloids and Surfaces A: Physicochemical and Engineering Aspects, 2024: 133462; https://doi.org/10.1016/j.colsurfa.2024.133462

[18] Zhou W, Zhan B, Wang G, et al., Separation and Purification Technology, 2024, 337: 126356; https://doi.org/10.1016/j.seppur.2024.126356

[19] Wu Y, Dong L, Ran Q., Applied Surface Science, 2024, 649: 159193; https://doi.org/10.1016/j.apsusc.2023.159193

[20] Diker C Ö, Duman O, Tunç S., Applied Clay Science, 2023, 244: 107109; https://doi.org/10.1016/j.clay.2023.107109

[21] Yang K, Wu Y, Gong X., Surface and Coatings Technology, 2023, 474: 130124; https://doi.org/10.1016/j.surfcoat.2023.130124

[22] Mastouri A, Efhamisisi D, Tarmian A, et al., Progress in Organic Coatings, 2024, 186: 107951; https://doi.org/10.1016/j.porgcoat.2023.107951

[23] Chang X, Yu H, Liu Z, et al., Colloids and Surfaces A: Physicochemical and Engineering Aspects, 2024, 684: 133188; https://doi.org/10.1016/j.colsurfa.2024.133188

[24] Bukit B F, Frida E, Humaidi S, et al., South African Journal of Chemical Engineering, 2022,

41: 105-110; https://doi.org/10.1016/j.sajce.2022.05.007

[25] Mallakpour S, Mohamma N., Carbohydrate Polymers, 2022, 285: 119226; https://doi.org/10.1016/j.carbpol.2022.119226

[26] Özdemir A O, Caglar B, Çubuk O, et al., Materials Chemistry and Physics, 2022, 287: 126342; https://doi.org/10.1016/j.matchemphys.2022.126342

[27] Luo Z, Zhang Z, Wang W, et al., Materials Chemistry and Physics, 2010, 119(1-2): 40-47; https://doi.org/10.1016/j.matchemphys.2009.07.039

[28] Fan Z, Wang D, Yuan Y, et al., Chemical Engineering Journal, 2020, 381: 122696; https://doi.org/10.1016/j.cej.2019.122696

[29] Gong X, Liu Y, Wang Y, et al., Polymer, 2019, 168: 131-137; https://doi.org/10.1016/j.polymer.2019.02.021

[30] Zhao J, Xie X, Zhang C., Corrosion Science, 2017, 114: 146-155; https://doi.org/10.1016/j.corsci.2016.11.007

[31] Neupane M P, Lee S J, Kang J Y, et al., Materials Chemistry and Physics, 2015, 163: 229-235; https://doi.org/10.1016/j.matchemphys.2015.07.034

[32] Zhao J, Xie X, Zhang C., Corrosion Science, 2017, 114: 146-155; https://doi.org/10.1016/j.corsci.2016.11.007

[33] Neupane M P, Lee S J, Kang J Y, et al., Materials Chemistry and Physics, 2015, 163: 229-235; https://doi.org/10.1016/j.matchemphys.2015.07.034

[34] Li B, Yin X, Xue S, et al., Applied Surface Science, 2022, 580: 152305; https://doi.org/10.1016/j.apsusc.2021.152305

[35] Qin L, Chu Y, Zhou X, et al., ACS applied materials & interfaces, 2019, 11(32): 29388-29395; https://doi.org/10.1021/acsami.9b07563

[36] Radziejewska J, Grzelka J., Polymer Testing, 2023, 117: 107866; https://doi.org/10.1016/j.polymertesting.2022.107866

[37] Yang Y, Zhang C, Hu Z., Environmental Science: Processes & Impacts, 2013, 15(1): 39-48; https://doi.org/10.1039/C2EM30655G